• Basic Research •

Modeling monocular form deprivation in rabbits using a simulated-cataract intraocular lens

Si–Yi Gu[1,2,3], Li–Ming Xu[1,2,3], Wei–Jie Sun[1,2,3], Li–Li Liang[1,2,3], Lei Lin[1,2,3], Han Zou[1,2,3], Jing–Yuan Xu[1,2,3], Yu Zheng[1,2,3], Yuan–Yuan Li[1,2,3], Yin–Ying Zhao[1,2,3], Ping–Jun Chang[1,2,3], Yun–E Zhao[1,2,3,4]

[1]Eye Hospital and School of Ophthalmology and Optometry, Wenzhou Medical University, Wenzhou 325003, Zhejiang Province, China
[2]The State Key Laboratory of Optometry, Ophthalmology and Vision Science, Wenzhou 325003, Zhejiang Province, China
[3]National Center for Clinical and Medical Research, Wenzhou 325003, Zhejiang Province, China
[4]Eye Hospital of Wenzhou Medical University at Hangzhou, Hangzhou 310000, Zhejiang Province, China
Co-first authors: Si-Yi Gu and Li-Ming Xu
Correspondence to: Yun-E Zhao. Eye Hospital of Wenzhou Medical University at Hangzhou, 618 East Fengqi Road, Hangzhou 310000, Zhejiang Province, China. zye@eye.ac.cn; zyehzeye@126.com
Received: 2023-02-26 Accepted: 2024-07-26

Abstract

● **AIM:** To establish an animal model of form deprivation amblyopia based on a simulated cataract intraocular lens (IOLs).

● **METHODS:** Poly(dimethyl siloxane)-SiO_2 thin films (PSF) with different degrees of opacity as IOL materials were prepared. The light transmission of the PSF-IOL was measured, and its *in vitro* biosafety was determined by cell counting kit (CCK)-8 assay using the HLEC-B3 cell line and ARPE-19 cell line. Subsequently, the *in vivo* safety was determined by implanting the PSF-IOL with 10% wt SiO_2 into the right eyes of New Zealand white rabbits (PSF-IOL group), and compared with two control groups: contralateral comparison group and normal control (NC) group (Contralateral comparison group: the fellow eye; NC group: a group of binocular normal rabbits without intervention). The flash visual-evoked potentials (F-VEPs) were measured to verify amblyopia.

● **RESULTS:** PSFs containing 0, 2%, and 10% wt SiO_2 were successfully constructed. The 0 SiO_2 PSF was transparent, while the 10% wt SiO_2 PSF was completely opaque. It was found that PSF did not induce unwanted cytotoxicity in HLECs and ARPE19 cells *in vitro*. *In vitro*, PSF-IOL with 10% wt SiO_2 was also non-toxic, and no significant inflammation or structural changes occurred after four weeks of PSF-IOL implantation. Finally, our IOL-simulated congenital cataract rabbit detected by F-VEPs suggested tentative amblyopia.

● **CONCLUSION:** A PSF-IOL that mimics cataracts is created. A novel form deprivation model is created by the IOL-simulated congenital cataract rabbit. It can be developed fast and stable and holds great potential for future study.

● **KEYWORDS:** monocular deprivation; form deprivation; intraocular lens; congenital cataract; amblyopia
DOI:10.18240/ijo.2024.12.04

Citation: Gu SY, Xu LM, Sun WJ, Liang LL, Lin L, Zou H, Xu JY, Zheng Y, Li YY, Zhao YY, Chang PJ, Zhao YE. Modeling monocular form deprivation in rabbits using a simulated-cataract intraocular lens. *Int J Ophthalmol* 2024;17(12):2177-2184

INTRODUCTION

Congenital cataracts are the leading cause of childhood blindness[1]. These can cause form deprivation amblyopia, which is the worst type of amblyopia[2]. Prior research has demonstrated structural alterations in the visual cortex, the lateral geniculate body, and ganglion cells of amblyopia animals, along with a reduction in synaptic density. Consequently, their functions continue to be impaired[3-5]. However, the microscopic mechanism of congenital cataracts causing form deprivation amblyopia remains largely unclear. In clinical practice, the severity of amblyopia varies because of various degree congenital cataracts. This diversity makes the study of the amblyopia mechanisms more complex. Thus, animal models simulating congenital cataracts of different severities may be a part of the solution.

From rodents to non-human primates, monocular deprivation has been widely used with varying degrees of success[6-8]. Currently, in the accepted animal model, monocular deprivation was induced with monocular eyelid sutures. In spite of its effectiveness, there is much difference between eyelid suturing-closure and congenital cataracts. Furthermore, eyelid suturing has a number of disadvantages. Eyelid suturing may cause eyelid infections, ulcerations and scarring, sometimes corneal ulceration, and intraocular pressure (IOP)

increasing, resulting modeling failure. Facemasks modified from latex balloons covering one eye could also lead to monocularly form-deprived animal models[8]. However, the mask can shift, resulting in unstable model-making.

By contrast, gene knockout cataract model should be a good form deprivation model[9]. However, gene knockout animals are often accompanied by abnormalities other than cataracts[10], such as microcornea, small-eye, and systemic abnormalities[10-12]. And these animals are often weak, making them susceptible to problems after the intervention. In this way, their survival rate will decrease, adding to the difficulty of the study. Moreover, gene knockout can also damage the animal's visual cortex, lateral geniculate body, or retina, resulting in interference with the research.

To establish a new model of form deprivation amblyopia, we designed an intraocular lens (IOL) that can simulate congenital cataracts with different degrees of opacity according to different formulations. SiO_2 is a non-toxic, widely used biomaterial that is also recognized as Generally Recognized As Safe (GRAS) by the U.S. Food and Drug Administration (FDA)[13-15]. It is a white powder. Poly (dimethyl siloxane) (PDMS) is also commonly used for foldable, colorless, and transparent IOLs because they are non-toxic, thermally and chemically stable, and inert to body fluids[16-17]. Thus, in this study, we mixed different wt% of SiO_2 with PDMS to make IOLs with different degrees of opacity. And the rabbits are highly sensitive to visual deprivation from the 25th day to the 40th day[18]. Thus, the critical period of visual development of rabbits should be between the 25th day to the 40th day. In this study, we used rabbits aged 21d and reared them for 4wk. We aim to establish an animal model of form deprivation amblyopia based on a simulated cataract IOL.

MATERIALS AND METHODS

Ethical Approval The experimental animal ethics application for this experiment (No.10409) was approved by the Committee of the Experimental Animal Center of Wenzhou Medical University. During the experiments, the investigators have always strictly adhered to the Statement of the Society for Research in Vision and Ophthalmology on the Use of Animals in Ophthalmology and Vision Research.

Preparation and Characterization of Simulated-Cataract IOLs

Preparation of the poly(dimethyl siloxane)-SiO_2 thin films PDMS was prepared using Sylgard®184 (Dow Corning, China)[19]. According to the producer's instructions, to prepare PDMS, elastomer base was combined with curing agent in a ratio of 10:1. For the poly(dimethyl siloxane)-SiO_2 thin films (PSF), different wt% of SiO_2 (ZM-SiO_2-1, Zhong Hang Zhong Mai, China) were added to the stirred mixture of the elastomer base and curing agent. A certain amount of the mixture was poured into a dish and sonicated for 10min to remove the air bubbles. After curing in a 60℃ oven for 12h, the blended films were peeled off and achieved a stable state. The film surface was then rinsed several times with phosphate-buffered saline (PBS; Solarbio, China) and deionized water until it was tack-free. To better fit the rabbit eye, a hole punch was used to create round films of PSF, which were 6 mm in diameter and 0.5 mm in thickness.

Evaluation of the clouding effect of the artificial lens Artificial lenses containing 0, 2%, and 10% wt SiO_2 were obtained, and the degree of opacity of artificial lenses with different wt% SiO_2 was evaluated using cameras.

Measurement of artificial lens transmission Light transmission studies were performed on the intraocular implants. The optical characteristics of the implants were evaluated using a ultraviolet–visible spectroscopy (UV-VIS) spectrophotometer. The transmission in the visible, infrared, and ultraviolet light ranges was measured (wavelength range of 200-800 nm). First, a flat sheet specimen of a suitable size was cut from different parts of the test specimen (PDMS+0 SiO_2, PDMS+10% SiO_2), placed into the colorimetric cell along the direction perpendicular to the incident light, and filled with PBS, which was used as the blank. Subsequently, the wavelength range of 200-800 nm was used for measurement, and the transmission of the test specimen was recorded.

In Vitro Cell Safety Assay of Intraocular Lens

Cell culture HLEC-B3 cell line (Genechem, Shanghai, China) and ARPE-19 cell line (Meilunbio, Suzhou, China) were cultured in a medium containing 10% fetal bovine serum (FBS; Gibco, Australia) and 90% DMEM/F12 (Gibco, USA). The cells were gently passaged at a ratio of 1:3 once they reached sub-confluence[20].

Cytotoxicity assay Leaching solutions were prepared to examine the cytotoxicity of PSF. Briefly, three PSF were placed in a 2 mL centrifuge tube and submerged in 1.5 mL PBS. A cytotoxicity test was conducted after shaking the leaching solutions for two days at 37℃[21].

After reaching 90% confluence, the cells were digested with trypsin-EDTA (0.25%). After centrifugation (1200 rpm for 4min), the single-cell suspension was used to calculate cell numbers using the Urine Sediment Counting Board (China)[22]. HLECs and ARPE-19 cells were seeded into 96-well tissue culture plates (Corning, USA) as the holder, and cell cultivation was conducted individually for 24h.

In the PSF-IOL groups, the primary culture medium was discarded and a new medium was added with 5% leaching solution and incubated for 1, 2, and 3d. Two control groups were used: one with 5% PBS (PBS control group) and one without (blank control group)[21]. The cell counting kit (CCK)-8 assay (Beyotime, China) was used to determine cell viability.

After washing the cells once with PBS, they were incubated for 2h with CCK-8 reagent. The optical density was then measured on a SpectraMax M5 microplate reader (Molecular Device, USA) at 450 nm[23].

***In Vivo* Animal Safety Assay**

Laboratory animal welfare Our studies were conducted on New Zealand white rabbits. The rabbits were provided by the Laboratory Animal Center of Wenzhou Medical University. They were raised and provided with adequate feed and water daily.

PSF implanted as rabbit intraocular lenses A total of 9 surgical rabbits (*n*=9) were included in this experiment. The right eyes of New Zealand white rabbits were the model groups with 10% SiO_2 PSF-IOL implantation, and the left eyes were the control groups. Using a small animal anesthesia machine, the rabbits were anesthetized with 4% isoflurane at 1.5 L/min. The rabbits were then continuously anesthetized with 2% isoflurane at a rate of 1.5 L/min.

All animals were operated on the right eye. The 3.0 mm limbal incision was made at the 11 o' clock position, and a viscoelastic agent was injected into the anterior chamber, followed by a continuous curvilinear capsulorhexis at approximately 5 mm. Next, water dissection was completed to fully rotate the lens nuclei. The soft nuclei and cortex were then removed using a manual irrigation/aspiration tube. Finally, PSF, a rabbit IOL, was implanted into the capsular bag. The incision was closed using 10-0 polypropylene sutures (Alcon, USA). Postoperative topical therapy consisted of tobramycin-dexamethasone ointment, prednisolone acetate drops, and levofloxacin eye drops, which were tapered in the first two weeks after surgery. The right eyes of rabbits that underwent surgery were in the PSF-IOL group. The left eye was the contralateral eye (contralateral comparison group). In addition, normal control rabbits without any intervention were set up as normal control (NC) group.

Slit lamp examination Simulating-cataract modeling (PSF-IOL group) success was determined by slit-lamp biomicroscopy examinations at four weeks postoperatively when compared with the contralateral comparison group. The IOLs' dense opacity and loss of red-light reflex are similar to natural cataracts, which meant simulating-cataract modeling success. Besides, slit lamp examination is also used to directly observe the resolution of inflammation.

Enzyme-linked immunosorbent assay to analyze cytokines Sterile insulin needles were used for aqueous humor extraction from the eyes after one week and four weeks of PSF-IOL implantation. Aqueous humor extraction was performed at the 9 o'clock limbus in the operated eyes and normal contralateral eyes. Approximately 80-100 μL of aqueous humor was collected from each eye. Enzyme-linked immunosorbent assay (ELISA) was conducted to calculate the concentration of pro-inflammatory cytokines interleukin (IL)-8 (Rabbit IL-8 ELISA Kit, SEKRT-0004, Solarbio, China) and tumor necrosis factor (TNF)-α (Rabbit TNF-α ELISA Kit, SEKRT-0402, Solarbio, China) in the aqueous humor of the eyes after one week and four weeks of IOL implantation. The absorbance of each well was measured at a wavelength of 450 nm.

Additionally, for the PSF-IOL group and contralateral comparison group, IOP was measured by a non-contact tonometer (TV01, icare TonoVet, Finland) at 0, 7, 14, and 28d post-operation.

***In vivo* animal visual function evaluation** We conducted experiments according to the protocol of the International Society for Clinical Visual Electrophysiology of Vision for standardizing clinical visual electrophysiological examination instruments (https://iscev.wildapricot.org/standards). Flash-visual evoked potentials (F-VEPs) were conducted on day 28 following IOL implantation with a Ganzfeld system (RetiPort, Roland Consult, Brandenburg, Germany).

Seven rabbits were randomly selected from the 9 operated rabbits for F-VEP tests. A total of 7 surgical rabbits (PSF-IOL and contralateral comparison group) and 6 normal rabbits (both eyes of NC group) were included to conduct F-VEPs. The settings of F-VEPs were according to the instructions, including full-field continuous white light, brightness of stimulus light: 4 cd/m^2, background light: 0 cd/m^2, flicker frequency: 2.0 Hz, low frequency: 0.1 Hz, high frequency: 85.0 Hz, and average test: 100 sweeps.

The working electrode was placed at the midpoint of the line connecting the front edges of the two ears of the rabbit. The reference electrode was put in the middle of the forehead, and the ground electrode was attached to the back. When examining one eye, its fellow eye was covered with foil stickers. The left eyes were tested first, then the right eyes.

We tested the latency of N1 and the amplitudes of P1 for each F-VEP wave and calculated the latency changes and Contralateral bias indices (CBI)[24] as follows: latency changes=latency of N1 of the right eyes/latency of N1 of the fellow left eyes; amplitude of P1=N1-P1; CBI=amplitude changes=amplitude of P1 of the right eyes/amplitude of P1 of the fellow left eyes.

Euthanasia and Histopathology Four weeks after PSF-IOL implantation, the rabbits were euthanized using an experimental animal asphyxiator (SMQ-II, Shanghai Mingli, China). Subsequently, both the right eyes (PSF-IOL group) containing PSF and the normal left eyes (contralateral comparison group) were taken for histological examination. The eyes were fixed in 4% formaldehyde, ethanol, distilled water, and acetic acid in a ratio of 1:4:4:1 for at least 48h at 4°C. After anatomical separation, ocular tissues, such as corneas and

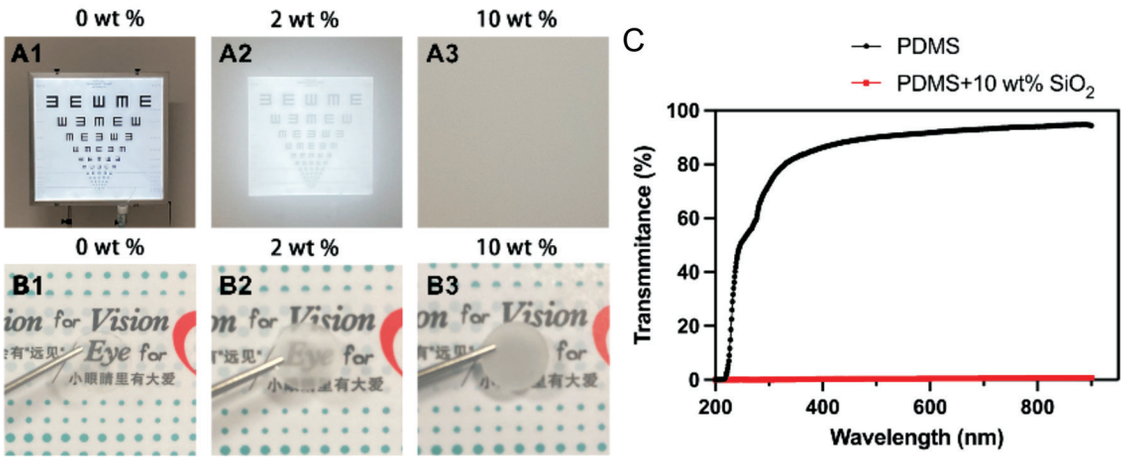

Figure 1 Blurred visions of IOLs containing different wt% of SiO_2 With IOLs covered the phone lens, shot 5 m away from the visual chart (A1-A3) and a forceps was used to place IOLs over the text and display the degree of opacity (B1-B3). PSF with a SiO_2 mass fraction of 0 results in clear visual chart and text (A1, B1); one with a SiO_2 mass fraction of 2% results in the slightly blurred visual chart and text (A2, B2); one with a 10% SiO_2 PSF results in completely unreadable visual chart and text (A3, B3). C: The transmission of the PSF (PDMS+0 SiO_2) in the visible, infrared, and ultraviolet light ranges was close to 100%, whereas that of the PSF (PDMS+10 SiO_2) was 0. PSF: Poly(dimethyl siloxane)-SiO_2 thin films; IOL: Intraocular lens; PDMS: Poly(dimethyl siloxane).

retinas, were dehydrated, embedded in paraffin, and sectioned on slides. All ocular tissues were cut into 5 μm thick tissue sections (HistoCore BIOCUT, Leica Biosystems, Nussloch, Germany). They were routinely conducted hematoxylin-eosin (HE) staining (Leica Autostainer XL-ST5010, Nussloch, Germany). Images were captured using an ECLIPSE Ni-U Upright Microscope (Nikon, Japan).

Statistical Analysis SPSS 26.0 was used to analyze the data, and the obtained data were presented as the means±standard deviations (SD). PRISM (GraphPad 8.0) was used to perform all statistical tests. A two-sample *t*-test was used to compare the results obtained from different samples under identical conditions. $P<0.05$ was considered statistically significant.

RESULTS

Characterization of the PSF To simulate monocular form deprivation with different levels of turbidity, we made PSF with 0, 2%, and 10% SiO_2. The 0 SiO_2 artificial lens provides a clear image of the text, a 2% SiO_2 artificial lens provides a slightly blurred image of the text, and a 10% SiO_2 artificial lens provides a completely illegible image of the text (Figure 1A, 1B). In addition, using a UV-VIS spectrophotometer, PSF (PDMS+0 SiO_2) was found to have close to 100% transmission in the visible, infrared, and ultraviolet light range, whereas PSF (PDMS+10% SiO_2) had zero transmission (Figure 1C). Therefore, it is possible to simulate different levels of monocular deprivation using PSFs with different degrees of opacity.

***In Vitro* Effect of the PSF on HLECs and ARPE-19 Cells** At the same incubation time (Figure 2A, 2B), HLECs and ARPE-19 cells in the leaching solution of IOL materials showed viability similar to that of the controls. This indicates that PSF did not induce unwanted cytotoxicity in HLECs and ARPE-19 cells *in vitro*.

Biosafety of PSF-IOL Implantation into Rabbit Eyes To further test the biosafety of PSF and examine the effects of monocular deprivation, we implanted IOLs containing 10% SiO_2 into the right eyes of New Zealand white rabbits (Figure 3A). We photographed the treated eye and the contralateral normal eye four weeks post-operation under slit light (Figure 3B1). and diffuse light (Figure 3B2). A slit-lamp imaging study revealed the accurate location of the IOLs in the capsular bag. In the normal contralateral comparison group, the reflection from the corneal surface of the slit lamp was transparent in all panels, whereas the IOLs of the PSF-IOL group exhibited dense opacities. The IOLs' dense opacity and loss of red-light reflex meant simulating-cataract modeling success. All operated eyes experienced mild inflammation during the first week, with mild corneal edema and iris inflammation near the corneal incision. Gradually, the inflammation subsided during weeks 2-4. Four weeks after the operation, no hyphema, corneal opacity, or corneal adhesion was observed (Figure 3B, 3C).

Additionally, after PSF implantation, IOP in the operated eyes decreased significantly in the first week but gradually returned to normal after the second week (Figure 4A). An ELISA was conducted to test the effects of PSF implantation on intraocular inflammation involving TNF-α and IL-8. In the first week following surgery, ELISA revealed a slight elevation in TNF-α (Figure 4B) and IL-8 ($P<0.05$; Figure 4C) levels in the aqueous humor of the PSF-IOL groups. However, four weeks later, the ELISA results of the PSF-IOL groups were consistent with those of the contralateral comparison group (Figure 4B, 4C). In

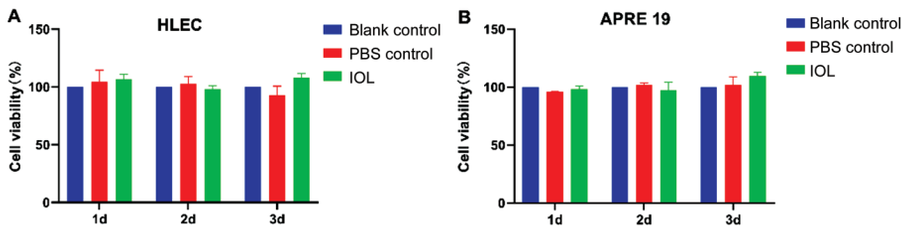

Figure 2 HLECs or ARPE-19 cells viability of the leaching solutions CCK-8 assay of HLECs (A) and ARPE-19 (B) cells co-cultured with 5% PSF leaching solutions (IOL group), 5% PBS (PBS control group) and normal medium (blank control group). CCK: Cell counting kit; PBS: Phosphate-buffered saline; PSF: Poly(dimethyl siloxane)-SiO^2 thin films; IOL: Intraocular lens.

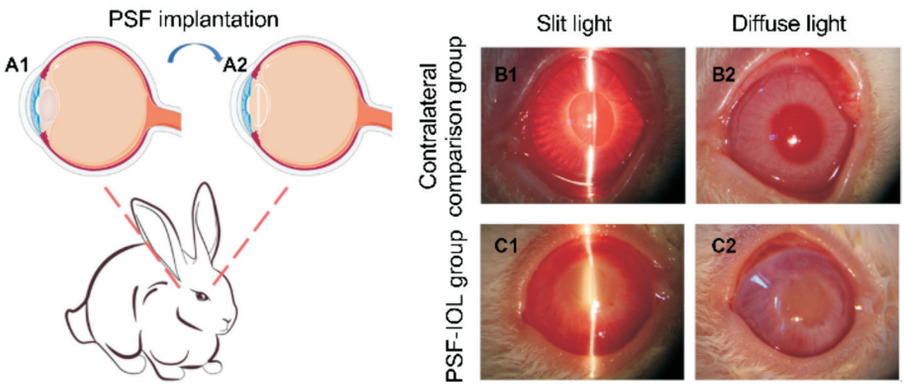

Figure 3 PSF implantation into the rabbit eye and slit-lamp images of contralateral comparison (*n*=9) and PSF-IOL groups (*n*=9) under slit and corresponding diffuse light A1-A2: Schematic illustration of the PSF implantation. B1-B2: Slit lamp photographs of the contralateral comparison group. B1 is the contralateral comparison group under slit light; B2 is the contralateral comparison group under diffuse light. C1-C2: Slit lamp photographs of the PSF-IOL group. C1 is the PSF-IOL group under slit light; C2 is the PSF-IOL group under diffuse light; PSF: Poly(dimethyl siloxane)-SiO_2 thin films; IOL: Intraocular lens.

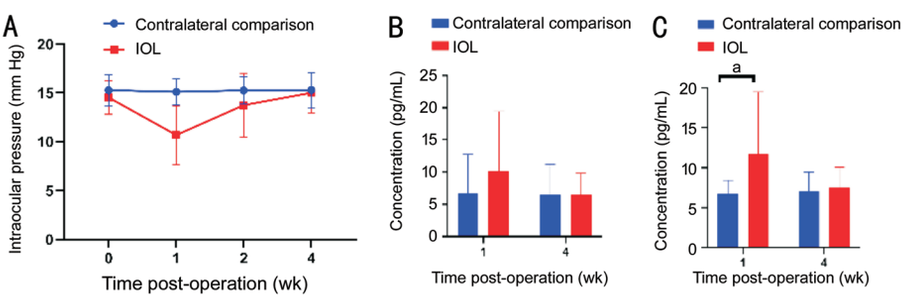

Figure 4 IOP and aqueous humor inflammatory factors following PSF implantation A: The IOP recordings revealed no significant differences between the contralateral comparison (*n*=9) and PSF-IOL groups (*n*=9) at 1 and 4wk post-operation. ELISA of inflammatory factors such as IL-8 (B) and TNF-α (C) in the aqueous humor of the contralateral comparison and PSF-IOL groups. [a]Statistically significant difference between the two groups. PSF: Poly(dimethyl siloxane)-SiO_2 thin films; IOL: Intraocular lens; IOP: Intraocular pressure; TNF-α: Tumor necrosis factor.

summary, PSF implantation in rabbit eyes did not cause severe inflammation or endophthalmitis.

Effect of PSF-IOL Implantation on Visual Function Examinations of F-VEPs were able to reflect visual function well. The F-VEP latency changes in the surgical rabbits (PSF-IOL and contralateral comparison group) were 111.08%±27.261%, and the F-VEP latency changes in the normal rabbits (NC group) were 99.44%±11.979%. It did not show any statistical significance between the two groups (Figure 5A). However, compared with the normal rabbits' CBI (103.75%±26.197%), the CBI was significantly lower (P<0.05; Figure 5B) in the surgical rabbits (64.56%±13.732%). These results implied that rabbits aged 21d developed amblyopia after 28d of monocular deprivation.

Effect of PSF-IOL Implantation on Ocular Histology To determine the effects of PSF-IOL implantation on ocular histology, rabbits were sacrificed four weeks after surgery. The eyeballs were enucleated, and the ocular tissues were cross-cut. The cornea and retina were stained with HE and examined microscopically. Compared with the contralateral comparison group, the PSF-IOL group retained normal histological characteristics. Normal layers can be identified in the cornea. Each layer of the retina exhibited normal morphology. Furthermore, no obvious apoptotic or necrotic cells were observed in the cornea or retina at 4wk post-operatively (Figure 6).

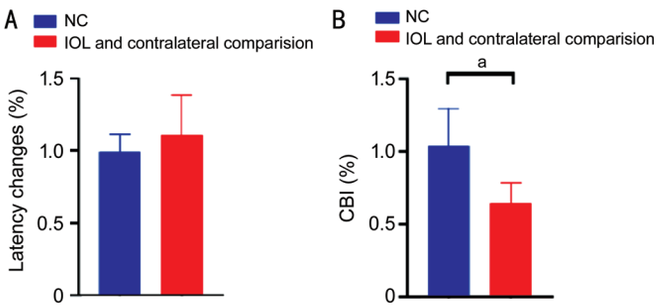

Figure 5 F-VEPs detection of New Zealand white rabbits at four weeks post-implantation A: No significant difference in latency changes between the surgical rabbits (contralateral comparison and PSF-IOL groups) and normal rabbits (both eyes of the NC group). B: Compared with the normal rabbits, the CBI in the surgical rabbits was significantly decreased (P<0.05). [a]The two groups of rabbits differed statistically significantly. CBI: Contralateral bias indices; PSF: Poly (dimethyl siloxane)-SiO_2 thin films; IOL: Intraocular lens; NC: Normal control.

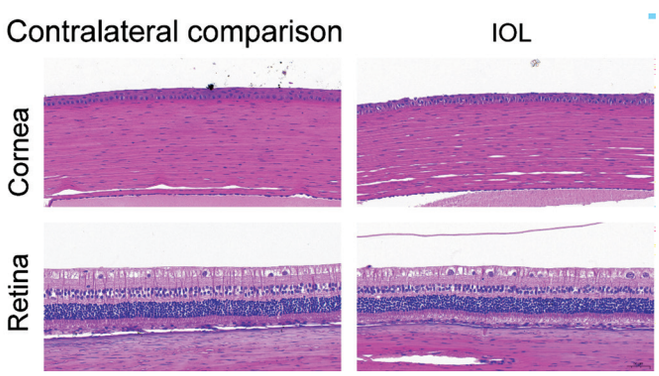

Figure 6 The HE staining of New Zealand white rabbit eyes demonstrating detailed histological identification of the cornea and retina in the contralateral comparison (n=9) and PSF-IOL groups (n=9) PSF: Poly (dimethyl siloxane)-SiO_2 thin films; IOL: Intraocular lens.

DISCUSSION

We developed IOLs that mimicked congenital cataracts. They provide a good stable model for the study of form-deprived amblyopia. It can make up for the shortcomings of eyelid sutures, masks and gene knockout cataract model.

An IOL is an artificial lens used in cataract surgery to replace natural lenses. Modern cataract surgery employs flexible and foldable IOLs made of silicone or acrylates[25]. Acrylic IOLs are most commonly used[26], which can be hydrophobic or hydrophilic (depending on their water content)[18]. In addition, the silicone material is widely used. In fact, only turbidity and biocompatibility must be considered when designing a simulated cataract IOL. Biomaterials, such as PDMS, are commonly used for foldable IOLs[16-17]. Thus, we used PDMS, a silicone material, mixed with SiO_2 to make IOLs with different degrees of turbidity to simulate congenital cataracts of different severities.

To test the biological safety of the IOL, we performed a series of experiments. For *in vitro* biosafety testing, we performed the cell experiments. As we all know, the cell experiments such as co-culture experiments and cell proliferation assays are classical ways to test cytotoxicity and biosafety before *in vivo* experiments. As the PSF-IOL material was newly synthesized, cell lines experiment *in vitro* were needed. In this study, we found that HLEC-B3 and ARPE-19 showed similar cell viability in the IOL group to the control group (PBS group and blank control group). This showed that PSF-IOL did not cause significant cytotoxicity to HLEC and ARPE-19 cells *in vitro*, and it had *in vitro* biosafety.

For the *in vivo* study, a monocular deprivation model was created using PSF (PDMS+10% SiO_2) implantation to simulate severe cataracts. Structure, function, and inflammatory parameters for biosafety research, such as aqueous humor tests, slit lamp, and visual function assay, and HE staining analysis for anatomical abnormalities, showed that IOLs made from PSF were biosafe and of clinical-grade quality.

For each animal, CBI indicates ocular dominance (OD) and a decrease in CBI means a shift in OD[24]. The non-dominant eye is more likely to develop amblyopia[27]. Thus, CBI is an important observation indicator for the development of amblyopia. It is reported that visual deprivation during the critical period of visual development shifts OD, leading to amblyopia[28-29]. We performed F-VEP for the rabbits and calculated the CBI to detect amblyopia. In order to eliminate variations in F-VEP amplitudes, the right eyes of each animal were compared with their fellow left eyes[30]. The F-VEP latency changes in the surgical rabbits and the normal rabbits (NC group) did not show any statistical significance (Figure 5A), as demonstrated in previous experiments[30]. The CBI was significantly lower (P<0.05; Figure 5B) in the surgical rabbits, which preliminarily demonstrated that our new congenital cataract rabbit model might have amblyopia[24,27,29,31-32].

Compared with gene knockout cataract model, our IOL-simulated congenital cataract rabbit model can prevent the occurrence of various systemic diseases[10], and it can be established in a short time. In addition, compared with the most recognized form deprivation amblyopia animal model induced by monocular eyelid suture, our model can solve the problems such as easy bleeding and line collapse[6]. Most importantly, this model can be used to simulate cataracts of different severities, and the degree of form deprivation can be controlled by using PSF-IOLs with different degrees of opacity.

Our study also has some limitations. We didn't test PSF-IOL *in vitro* and *in vivo* with varying degrees of opacity. However, we suspect that PSF with different SiO_2 mass fractions has no impact on toxicity and biocompatibility testing. Moreover, IOL implantation is an invasive procedure that can do more or less harm to the animals, such as postoperative inflammation. Given

that this technique is common and safe, the inflammation can be effectively treated with eye drops in a short time.

In summary, PSF was prepared by adding different mass percentages of SiO_2 into the stirring solution of the elastomer binder and curing agent for making PDMS. A PSF-IOL that mimics cataract was created. Then a novel form deprivation model was created by IOL-simulated congenital cataract rabbit. It can be developed fast and stable and holds great potential for future study. Further applications of this novel animal model are expected to investigate the relationship between different severities of form deprivation and amblyopia and the underlying microscopic mechanisms behind amblyopia.

ACKNOWLEDGEMENTS

Foundation: Supported by National Natural Science Foundation of China (No.81870680).

Conflicts of Interest: Gu SY, None; **Xu LM,** None; **Sun WJ,** None; **Liang LL,** None; **Lin L,** None; **Zou H,** None; **Xu JY,** None; **Zheng Y,** None; **Li YY,** None; **Zhao YY,** None; **Chang PJ,** None; **Zhao YE,** None.

REFERENCES

1 Hensch TK, Quinlan EM. Critical periods in amblyopia. *Vis Neurosci* 2018;35:E014.

2 Park SH. Current management of childhood amblyopia. *Korean J Ophthalmol* 2019;33(6):557-568.

3 Kiorpes L. Understanding the development of amblyopia using macaque monkey models. *Proc Natl Acad Sci U S A* 2019;116(52): 26217-26223.

4 Xu LM, Li ZG, Rong JB, Lang LJ. Effect of regulation of the NRG1/ErbB4 signaling pathway on the visual cortex synaptic plasticity of amblyopic adult rats. *J Biochem Mol Toxicol* 2021;35(9):e22841.

5 Bi AL, Zhang YY, Lu ZY, Tang HY, Zhang XY, Zhang ZH, Li BQ, Guo DD, Gong S, Li Q, Wang XR, Lu XZ, Bi HS. Synaptosomal actin dynamics in the developmental visual cortex regulate behavioral visual acuity in rats. *Invest Ophthalmol Vis Sci* 2021;62(7):20.

6 Murase S, Robertson SE, Lantz CL, Liu J, Winkowski DE, Quinlan EM. Chronic monocular deprivation reveals MMP9-dependent and-independent aspects of murine visual system plasticity. *Int J Mol Sci* 2022;23(5):2438.

7 Mikhailova GZ, Shtanchaev RS, Bezgina EN, Kashirskaya NN, Pen'kova NA, Tiras NR. Changes in the dendrite morphology of mauthner neurons in goldfish under the conditions of monocular deprivation and sensory stimulation. *Biophysics* 2019;64(1):67-74.

8 Tian L, Guo YT, Ying M, Liu YC, Li X, Wang Y. Co-existence of myopia and amblyopia in a guinea pig model with monocular form deprivation. *Ann Transl Med* 2021;9(2):110.

9 Li JY, Chen XJ, Yan YB, Yao K. Molecular genetics of congenital cataracts. *Exp Eye Res* 2020;191:107872.

10 Bremond-Gignac D, Daruich A, Robert MP, Valleix S. Recent developments in the management of congenital cataract. *Ann Transl Med* 2020;8(22):1545.

11 Reis LM, Semina EV. Genetic landscape of isolated pediatric cataracts: extreme heterogeneity and variable inheritance patterns within genes. *Hum Genet* 2019;138(8-9):847-863.

12 Shiels A, Hejtmancik JF. Mutations and mechanisms in congenital and age-related cataracts. *Exp Eye Res* 2017;156:95-102.

13 Zhang Y, Hsu BYW, Ren CL, Li X, Wang J. Silica-based nanocapsules: synthesis, structure control and biomedical applications. *Chem Soc Rev* 2015;44(1):315-335.

14 Alvarez Echazú MI, Perna O, Olivetti CE, Antezana PE, Municoy S, Tuttolomondo MV, Galdopórpora JM, Alvarez GS, Olmedo DG, Desimone MF. Recent advances in synthetic and natural biomaterials-based therapy for bone defects. *Macromol Biosci* 2022;22(4):e2100383.

15 Saini RS, Binduhayyim RIH, Gurumurthy V, Alshadidi AAF, Aldosari LIN, Okshah A, Kuruniyan MS, Dermawan D, Avetisyan A, Mosaddad SA, Heboyan A. Dental biomaterials redefined: molecular docking and dynamics-driven dental resin composite optimization. *BMC Oral Health* 2024;24(1):557.

16 Shin MK, Ji YW, Moon CE, Lee H, Kang B, Jinn WS, Ki J, Mun B, Kim MH, Lee HK, Haam S. Matrix metalloproteinase 9-activatable peptide-conjugated hydrogel-based fluorogenic intraocular-lens sensor. *Biosens Bioelectron* 2020;162:112254.

17 Wu QN, Liu D, Chen W, Chen H, Yang C, Li XL, Yang CD, Lin HT, Chen SY, Hu N, Chen WR, Xie X. Liquid-like layer coated intraocular lens for posterior capsular opacification prevention. *Appl Mater Today* 2021;23:100981.

18 Sen P, Kshetrapal M, Shah C, Mohan A, Jain E, Sen A. Posterior capsule opacification rate after phacoemulsification in pediatric cataract: hydrophilic versus hydrophobic intraocular lenses. *J Cataract Refract Surg* 2019;45(10):1380-1385.

19 Paunović N, Leroux JC, Bao YY. 3D printed elastomers with Sylgard-184-like mechanical properties and tuneable degradability. *Polym Chem* 2022;13(16):2271-2276.

20 Lin L, Lin QK, Li J, Han YM, Chang PJ, Lu F, Zhao YE. ROCK inhibitor modified intraocular lens as an approach for inhibiting the proliferation and migration of lens epithelial cells and posterior capsule opacification. *Biomater Sci* 2019;7(10):4208-4217.

21 Lin QK, Tang JM, Han YM, Xu X, Hao XJ, Chen H. Hydrophilic modification of intraocular lens *via* surface initiated reversible addition-fragmentation chain transfer polymerization for reduced posterior capsular opacification. *Colloids Surf B Biointerfaces* 2017;151:271-279.

22 Zhang XB, Wang J, Xu JW, Xu W, Zhang Y, Luo CQ, Ni S, Han HJ, Shentu XC, Ye J, Ji J, Yao K. Prophylaxis of posterior capsule opacification through autophagy activation with indomethacin-eluting intraocular lens. *Bioact Mater* 2023;23:539-550.

23 Liu JJ, Dong YR, Ji QS, Wen YC, Ke GJ, Shi L, Guan W, Xu WP. Circ-MKLN1/miR-377-3p/CTGF axis regulates the TGF-β2-induced posterior capsular opacification in SRA01/04 cells. *Curr Eye Res* 2022;47(3):372-381.

24 Pulimood NS, Rodrigues WDSJ, Atkinson DA, Mooney SM, Medina AE. The role of CREB, SRF, and MEF2 in activity-dependent neuronal plasticity in the visual cortex. *J Neurosci* 2017;37(28): 6628-6637.

25 Chaniecki P, Stodolak-Zych E, Cholewa-Kowalska K, Rękas M. Evaluation of long-term changes in physicochemical properties of hydrophobic intraocular lenses in a laboratory model. *Ophthalmol J* 2022;7:176-187.

26 Topete A, Saramago B, Serro AP. Intraocular lenses as drug delivery devices. *Int J Pharm* 2021;602:120613.

27 Coren S, Duckman RH. Ocular dominance and amblyopia. *Am J Optom Physiol Opt* 1975;52(1):47-50.

28 Murphy EH, Magness R. Development of the rabbit visual cortex: a quantitative Golgi analysis. *Exp Brain Res* 1984;53(2): 304-314.

29 Mitchell DE, Maurer D. Critical periods in vision revisited. *Annu Rev Vis Sci* 2022;8:291-321.

30 Touitou V, Johnson MA, Guo Y, Miller NR, Bernstein SL. Sustained neuroprotection from a single intravitreal injection of PGJ2 in a rodent model of anterior ischemic optic neuropathy. *Invest Ophthalmol Vis Sci* 2013;54(12):7402-7409.

31 Wildberger H, Hofmann H, Siegfried J. Fluctuations of visual evoked potential amplitudes and of contrast sensitivity in Uhthoff's symptom. *Doc Ophthalmol* 1987;65(3):357-365.

32 Mitchell D, Sengpiel F. Animal models of amblyopia. *Vis Neurosci* 2018;35:E017.